

IBD Meta-analysis

Taylor Reiter Luiz Irber ... Phillip Brooks Alicia Gingrich
C. Titus Brown

June 3, 2020

Introduction

Metagenomics captures the functional potential of microbial communities through DNA sequencing of genes and organisms. Metagenomics has been used to profile many human microbial communities, including those that change in or contribute to disease. In particular, human gut microbiomes have been extensively characterized for their potential role in diseases such as obesity (Greenblum, Turnbaugh, and Borenstein 2012), type II diabetes (Qin et al. 2012), colorectal cancer (Wirbel et al. 2019), and inflammatory bowel disease (Lloyd-Price et al. 2019; Morgan et al. 2012; Hall et al. 2017; Franzosa et al. 2019). Inflammatory bowel disease (IBD) refers to a spectrum of diseases characterized by chronic inflammation of the intestines and is likely caused by host-mediated inflammatory responses at least in part elicited by microorganisms (Kostic, Xavier, and Gevers 2014). However, no causative or consistent microbial signature has been associated with IBD to date.

Statements about biology, determined once computation is all done

Although there is no consistent taxonomic or functional trend in the gut microbiome associated with IBD diagnosis, metagenomic studies conducted unto this point have left substantial portions of data unanalyzed. Reference-based pipelines commonly used to analyze metagenomic data from IBD cohorts such as HUMANN2 characterize on average 31%-60% of reads from the human gut microbiome metagenome, as many reads do not closely match sequences in reference databases (Franzosa et al. 2014; Lloyd-Price et al. 2019). To combat this issue, reference-free approaches like *de novo* assembly and binning are used to generate metagenome-assembled genome bins (MAGs) that represent species-level composites of closely related organisms in a sample. However, *de novo* approaches fail when there is low-coverage of or high strain variation in gut microbes, or with sequencing error (Olson et al. 2017). Even when performed on a massive scale, an average of 12.5% of reads fail to map to all *de novo* assembled organisms from human microbiomes (Pasolli et al. 2019).

Here we perform a meta-analysis of six studies of IBD gut metagenome cohorts comprising 260 CD, 132 UC and 213 healthy controls (see **Table 1**) (Lloyd-Price et al. 2019; Lewis et al. 2015; Hall et al. 2017; Franzosa et al. 2019; Gevers et al. 2014; Qin et al. 2010). First, we re-analyzed each study using a consistent k-mer-based, reference-free approach. We demonstrate that diagnosis accounts for a small but significant amount of variation between samples. Next, we used random forests to predict IBD diagnosis and to determine the k-mers that are predictive of UC and CD. Then, we use compact de Bruijn graph queries to reassociate k-mers with sequence context and perform taxonomic and functional characterization of these sequence neighborhoods. We find that strain variation is important (ADD MORE HERE AFTER CORNCOB). Our analysis pipeline is lightweight and is extensible to other association studies in large metagenome sequencing cohorts.

Results

Table 1: Six IBD cohorts used in this meta-analysis.

Cohort	Cohort names	Country	Total	CD	UC	nonIBD	Reference
iHMP	IBDMDB	USA	106	50	30	26	(Lloyd-Price et al. 2019)
PRJEB2054	MetaHIT	Denmark, Spain	124	4	21	99	(Qin et al. 2010)
SRP057027	NA	Canada, USA	112	87	0	25	(Lewis et al. 2015)
PRJNA385949	PRISM, STiNKi	USA	17	9	5	3	(Hall et al. 2017)
PRJNA400072	PRISM, LLDeep, and NLIBD	USA, Netherlands	218	87	76	55	(Franzosa et al. 2019)
PRJNA237362	RISK	North America	28	23	0	5	(Gevers et al. 2014)
Total			605	260	132	213	

Annotation-free approach for meta-analysis of IBD metagenomes.

Given that both reference-based and *de novo* methods suffer from substantial and biased loss of information in the analysis of metagenomes (Thomas and Segata 2019; Breitwieser, Lu, and Salzberg 2019), we sought a reference- and assembly-free pipeline to fully characterize each sample (Figure 1). K-mers, words of length k in nucleotide sequences, have previously been exploited for annotation-free characterization of sequencing data (reviewed by Rowe (2019)). K-mers are suitable for metagenome analysis because they do not need to be present in reference databases to be included in analysis and because they capture information from reads even when there is low coverage or high strain variation that preclude assembly. In particular, scaled MinHash sketching produces compressed representations of k-mers in a metagenome while retaining the sequence diversity in a sample (Pierce et al. 2019). Importantly, this approach creates a consistent set of hashes across samples by retaining the same hashes when the same k-mers are observed. This enables comparisons between metagenomes. Given these attributes, we use scaled MinHash sketches to perform metagenome-wide k-mer association with IBD-subtype. We refer to the scale MinHash sketches as *signature*, and to each subsampled k-mer in a signature as a *hash*.

We also implemented a consistent preprocessing pipeline to remove erroneous sequences that could falsely deflate similarity between samples. We removed adapters, human DNA, and erroneous k-mers, and filtered signatures to retain hashes that were present in multiple signatures. These preprocessing steps removed hashes that were likely to be errors while keeping hashes that were real but of low abundance in some signatures. 7,376,151 hashes remained after preprocessing and filtering.

K-mers capture variation due to disease subtype

In this study, we aimed to identify microbial signatures associated with IBD. However, given that biological and technical artifacts can differ greatly between metagenome studies (Wirbel et al. 2019), we first quantified these sources of variation. We calculated pairwise distance matrices using jaccard distance and cosine distance between filtered signatures, where jaccard distance captured sample richness and cosine distance captured sample diversity. We performed principle coordinate analysis and PERMANOVA with these distance matrices (Figure 2), using the variables study accession, diagnosis, library size, and number of hashes in a filtered signature (Table 2). Number

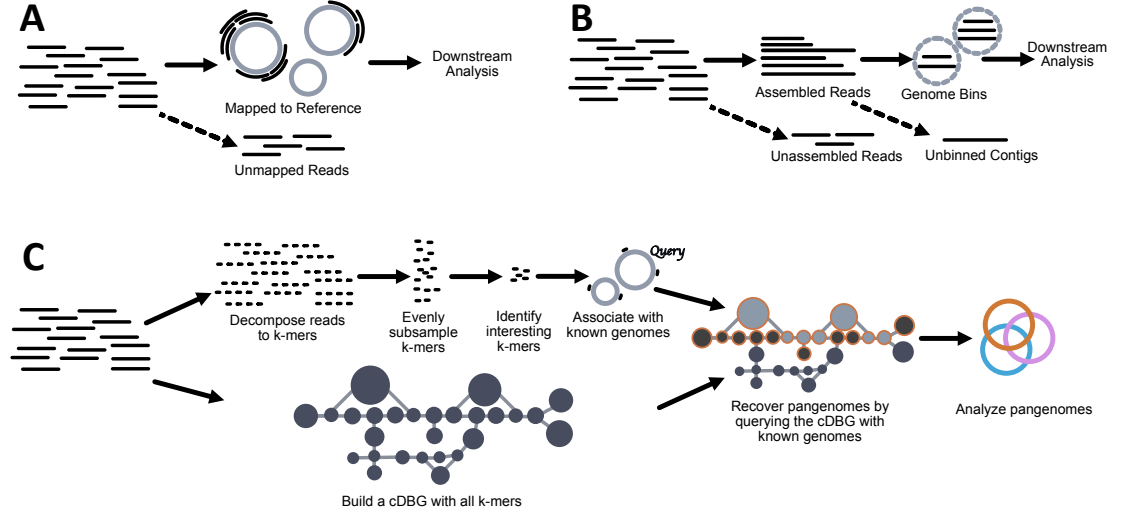


Figure 1: Comparison of common metagenome analysis techniques with the method used in this paper. Metagenomes consist of short (~ 50 - 300 bp) reads derived from sequencing DNA from environmental samples. **A** Reference-based metagenomic analysis. Reads are compared to genomes, genes, or proteins in reference databases to determine the presence and abundance of organisms and proteins in a sample. Unmapped reads are typically discarded from downstream analysis. **B** *De novo* metagenome analysis. Overlapping reads are assembled into longer contiguous sequences (~ 500 bp- 150 kbp, (Vollmers, Wiegand, and Kaster 2017)) and binned into metagenome-assembled genome bins. Bins are analyzed for taxonomy, abundance, and gene content. Reads that fail to assemble and contigs that fail to bin are usually discarded from downstream analysis. **C** Annotation-free approach for meta-analysis of metagenomes. We decompose reads into k-mers and subsample these k-mers, selecting k-mers that evenly represent the sequence diversity within a sample. We then identify interesting k-mers using random forests, and associate these k-mers with genomes in reference databases. Meanwhile, we construct a compact de Bruijn graph (cDBG) that contains all k-mers from a metagenome. We query this graph with known genomes that contain our interesting k-mers to recover sequence diversity nearby our query sequences in the cDBG. In the colored cDBG, light grey nodes indicate nodes that contain at least one identical k-mer to the query, while nodes outlined in orange indicate the nearby sequences recovered via cDBG queries. The combination of all orange nodes produces a sample-specific pangenome that represents the strain variation of closely-related organisms within a single metagenome. We repeat this process for all metagenomes and generate a single pangenome depicted in orange, blue, and pink.

of hashes in a filtered signature accounts for the highest variation, possibly reflecting reduced diversity in stool metagenomes of CD and UC patients (reviewed in (Schirmer et al. 2019)). Study accounts for the second highest variation, emphasizing that technical artifacts can introduce biases with strong signals. Diagnosis accounts for a similar amount of variation as study, demonstrating that there is a small but detectable signal of IBD subtype in stool metagenomes.

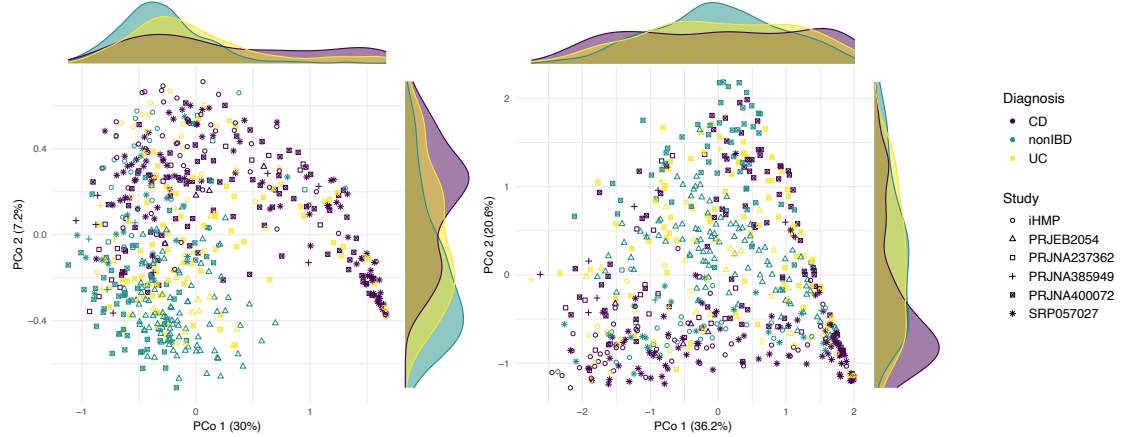


Figure 2: Principle coordinate analysis of metagenomes from IBD cohorts performed on filtered signatures. **A** Jaccard distance. **B** Angular distance.

Table 2: Results from PERMANOVA performed on Jaccard and Angular distance matrices. Number of hashes refers to the number of hashes in the filtered signature, while library size refers to the number of raw reads per sample. * denotes $p < .001$.

Variable	Jaccard distance	Angular distance
Number of hashes	9.9%*	6.2%*
Study accession	6.6%*	13.5%*
Diagnosis	6.2%*	3.3%*
Library size	0.009%*	0.01%*

Hashes are weakly predictive of IBD subtype

To evaluate whether the variation captured by diagnosis is predictive of IBD disease subtype, we built random forests classifiers to predict CD, UC, or non-IBD. We selected random forests because of the interpretability of feature importance via variable importance measurements. We used a leave-one-study-out cross-validation approach where we built and optimized a classifier using five cohorts and validated on the sixth.

Given the high-dimensional structure of this dataset (e.g. many more hashes than samples), we first used the vita method to select predictive hashes in the training set (Janitza, Celik, and Boulesteix 2018; Degenhardt, Seifert, and Szymczak 2017). Vita variable selection is based on permutation of variable importance, where p-values for variable importance are calculated against a null distribution that is built from variables that are estimated as non-important (Janitza, Celik, and Boulesteix 2018). This approach retains important variables that are correlated (Janitza, Celik, and Boulesteix 2018; Seifert, Gundlach, and Szymczak 2019), which is desirable in omics-settings where correlated features are often involved in a coordinated biological response, e.g. part of the same operon, pathways, or genome (Stuart et al. 2003; Sabatti et al. 2002). Variable selection reduced the number of hashes used in each model to 29,264-41,701 (Table

91 **3**). Using this reduced set of hashes, we then optimized each random forests classifier on the
 92 training set, producing six optimized models. We validated each model on the left-out study.
 93 The accuracy on the validation studies ranged from 49.1%-75.9% (**Figure 3**), outperforming a
 94 previously published model built on metagenomic data alone (Franzosa et al. 2019).

Table 3: Number of hashes retained after Vita variable selection for each of 6 classifiers. Classifiers are labelled by the validation study that was held out from training.

Validation study	Selected hashes
iHMP	39628
PRJEB2054	35343
PRJNA237362	40726
PRJNA385949	41701
PRJNA400072	32578
SRP057027	29264

95 We next sought to understand whether there was a consistent biological signal captured among
 96 classifiers by evaluating the fraction of shared hashes selected by variable selection between models.
 97 We intersected each set of hashes used to build each optimized classifier (**Figure 3**). Nine hundred
 98 thrity two hashes were shared between all classifiers, while 3,859 hashes were shared between at
 99 least five studies. The presence of shared hashes between classifiers indicates that there is a weak
 100 but consistent biological signal for IBD subtype between cohorts.

101 Shared hashes accounted for 2.8% of all hashes used to build the optimized classifiers. If shared
 102 hashes are predictive of IBD subtype, we would expect that these hashes would account for an
 103 outsized proportion of variable importance in the optimized classifiers. To calculate the relative
 104 variable importance contributed by each hash, we first normalized the variable importance values
 105 within each classifier by dividing by the total variable importance (e.g. sum to 1 within each
 106 classifier). We then normalized the variable importance across all classifiers by dividing by the
 107 total number of classifiers (e.g. divided by six so the total variable importance of all hashes across
 108 all classifiers summed to 1). 40.2% of the total variable importance was held by the 3,859 hashes
 109 shared between at least five classifiers, with 21.5% attributable to the 932 hashes shared between
 110 all six classifiers. This indicates that shared hashes contribute a large fraction of predictive power
 111 for classification of IBD subtype.

112 Some predictive hashes anchor to known genomes

113 We next evaluated the identity of the predictive hashes in each classifier. We first compared
 114 the predictive hashes against sequences in reference databases. We used sourmash **gather** to
 115 anchor predictive hashes to known genomes (Pierce et al. 2019). We compared our predictive
 116 hashes against all microbial genomes in GenBank, as well as metagenome-assembled genomes
 117 from three recent *de novo* assembly efforts from human microbiome metagenomes (Pasolli et al.
 118 2019; Nayfach et al. 2019; Almeida et al. 2019). Between 75.1-80.3% of hashes anchored to 1,161
 119 genomes (**Figure 4**). This indicates that 19.7-24.9% of hashes that are predictive of IBD subtype
 120 represent sequences not in reference databases.

121 The 3,859 hashes shared between at least five classifiers anchored to only 41 genomes (**Figure 4**).
 122 Futher, these 41 genomes accounted for 50.5% of the total variable importance, a 10.3% increase
 123 over the hashes alone. This means that tehse genomes contain additional predictive hashes not
 124 shared between at least five classifiers.

125 In contrast to all hashes, only 69.4% of these hashes were identifiable among the 3,859 shared

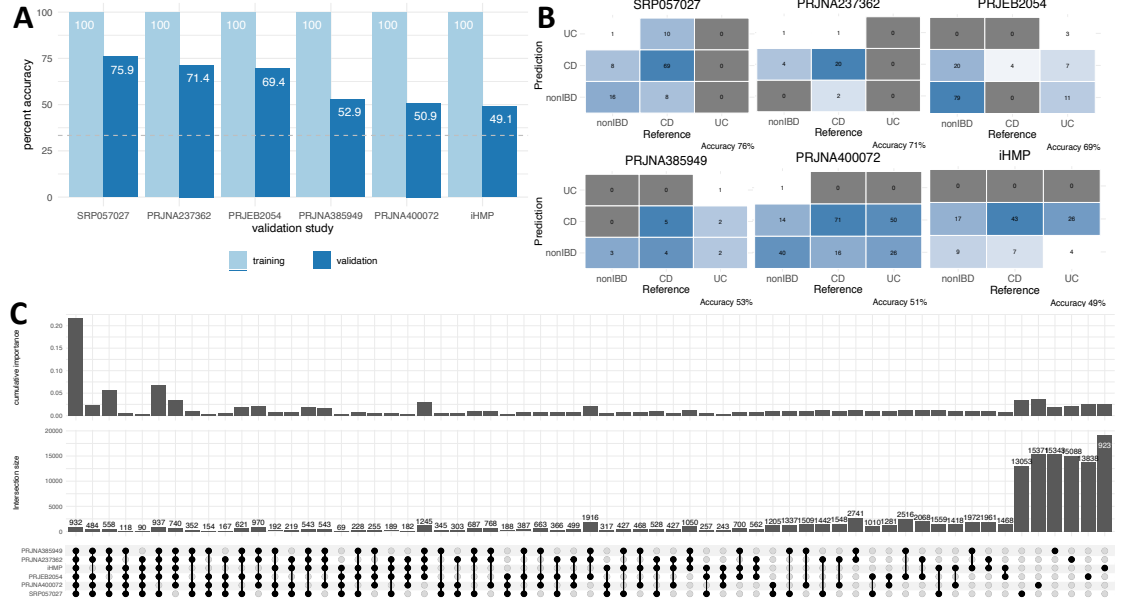


Figure 3: Random forest classifiers weakly predict IBD subtype. **A** Accuracy of leave-one-study-out random forest classifiers on training and validation sets. The validation study is on the x axis. **B** Confusion matrices depicting performance of each leave-one-study-out random forest classifier on the validation set. **C** Upset plot depicting intersections of sets of hashes as well as the cumulative normalized variable importance of those hashes in the optimized random forest classifiers. Each classifier is labelled by the left-out validation study.

126 hashes, a decrease of 5.7-10.9%. This indicates that hashes that are more likely to be important
 127 for IBD subtype classification are less likely to be anchored to genomes in reference databases.

128 Using sourmash lca classify to assign GTDB taxonomy, we find 38 species represented among
 129 the 41 genomes. The genome that anchors the most variable importance is **Acetatifactor**
 130 **sp900066565**. (Add %phyla/etc? Is it even worth analyzing these that much when everything
 131 changes after spacegraphcats?) However, we observe that while most genomes assign to one
 132 species, 19 assign to an additional one or more distantly related genomes that likely represent
 133 contamination from the assembly and binning process. When we take the Jaccard index of these 41
 134 genomes, we observe little similarity despite contamination (**Figure 4**). Therefore, we proceeded
 135 with analysis with the idea that each of the 41 genomes is a self-contained entity that captures
 136 distinct biology.

137 Unknown but predictive hashes represent novel pangenomic elements

138 Given that 30.6% of hashes shared between at least five classifiers did not anchor to genomes
 139 in databases, we next sought to characterize these hashes. We reasoned that many unknown
 140 but predictive hashes likely originate from closely related strain variants of identified genomes
 141 and sought to recover these variants. We performed compact de Bruijn graph queries into
 142 each metagenome sample with the 41 genomes that contained predictive hashes (CITATION:
 143 SPACEGRAPHCATS). This produced pangenome neighborhoods for each of the 41 genomes.
 144 86.1% of hashes shared between at least five classifiers were in the pangenomes of the 41 genomes,
 145 a 16.7% increase over the 41 genomes alone. This suggests that at least 16.7% of shared hashes
 146 originate from novel strain-variable or accessory elements in pangenomes.

147 Further, these pangenomes captured an additional 4.2-5.2% of all predictive hashes from each
 148 classifier, indicating that pangenomes contain novel sequences not captured in any database

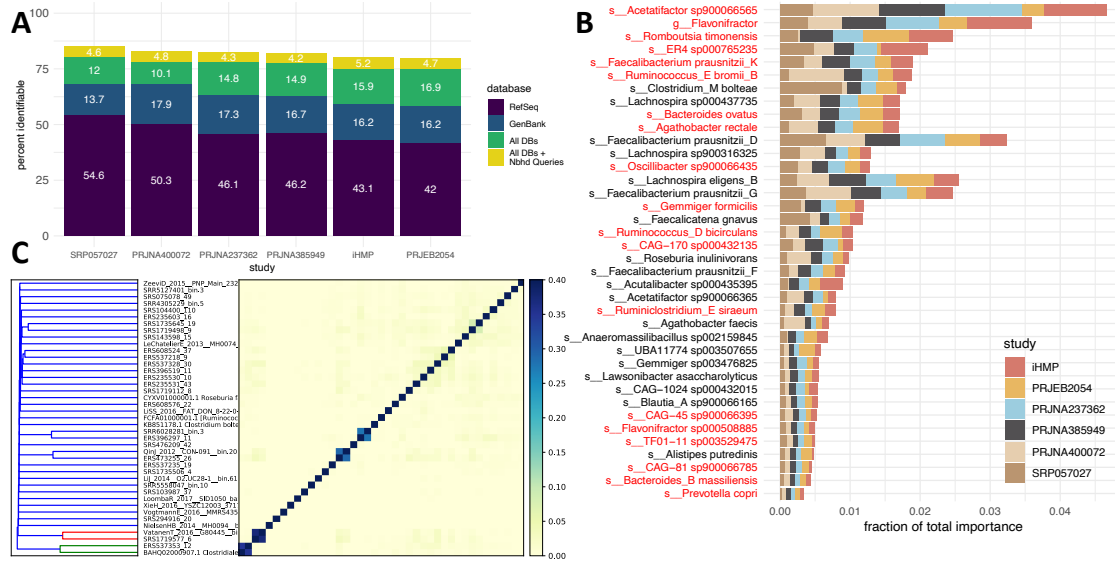


Figure 4: Some predictive hashes from random forest classifiers anchor to known genomes. **A** 75.1-80.3% of all hashes used to train classifiers anchor to known genomes in RefSeq, GenBank, or human microbiome metagenome-assembled genome databases. A further 4.2-5.6% of hashes anchor to pangenomes of a subset of these genomes. **B** The 3,859 hashes shared between at least five classifiers anchor to 41 genomes. Genomes account for different amounts of variable importance in each model. Genomes are labelled by 38 GTDB taxonomy assignments. Genomes labelled in red were classified as multiple distantly related species, likely indicating contamination. **C** Jaccard similarity between 41 genomes. The highest similarity between genomes is 0.37 and is shared by genomes of the same species, while most genomes have no similarity. This indicates that each genome represents distinct nucleotide sequence.

(Figure 4). The pangenomes also captured 74.5% of all variable importance, a 24% increase over the 41 genomes alone. This indicates that pangenomic variation contributes substantial predictive power toward IBD subtype classification.

Pangenomic neighborhood queries disproportionately impact the variable importance attributable to specific genomes (Figure 5). While most genomes maintained a similar proportion of importance with or without pangenome queries, three pangenomes shifted dramatically. While an *Acetatifactor* species anchored the most importance prior to pangenome construction, the specific species of *Acetatifactor* switched from *sp900066565*, to *sp900066365*. Conversely, *Faecalibacterium prausnitzii_D* increased from anchoring ~2.9% to ~10.5% of the total variable importance. These results indicate that strain variation is more important and less characterizable for prediction of IBD subtype in some species that in others.

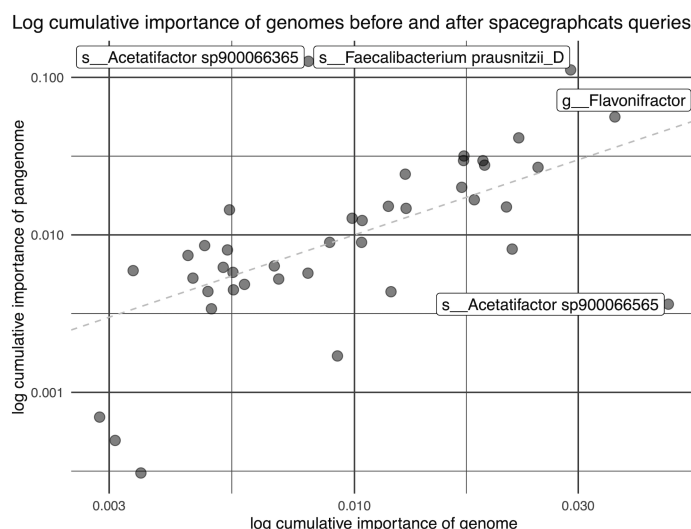


Figure 5: Pangenome neighborhoods generated with cDBG queries recover strain variation that is important for predicting IBD subtype. While the variable importance attributable to some genomes does not change with cDBG queries, other genomes increase by more than 7%.

Differential Abundance of Pangenomes

TBD

Discussion

Methods

All code associated with our analyses is available at www.github.com/dib-lab/2020-ibd/

IBD metagenome data acquisition and processing

We searched the NCBI Sequence Read Archive and BioProject databases for shotgun metagenome studies that sequenced fecal samples from humans with Crohn’s disease, ulcerative colitis, and healthy controls. We included studies sequenced on Illumina platforms with paired-end chemistries and with sample libraries that contained greater than one million reads. For time series intervention

cohorts, we selected the first time point to ensure all metagenomes came from treatment-naive subjects.

We downloaded metagenomic fastq files from the European Nucleotide Archive using the “fastq_ftp” link and concatenated fastq files annotated as the same library into single files. We also downloaded iHMP samples from idbmdb.org. We used Trimmomatic (version 0.39) to adapter trim reads using all default Trimmomatic paired-end adapter sequences (ILLUMINACLIP:{inputs/adapters.fa}:2:0:15) and lightly quality-trimmed the reads (MINLEN:31 LEADING:2 TRAILING:2 SLIDINGWINDOW:4:2) (Bolger, Lohse, and Usadel 2014). We then removed human DNA using BBDMap and a masked version of hg19 (Bushnell 2014). Next, we trimmed low-abundance k-mers from sequences with high coverage using khmer’s `trim-low-abund.py` (Crusoe et al. 2015).

Using these trimmed reads, we generated scaled MinHash signatures for each library using sourmash (k-size 31, scaled 2000, abundance tracking on) (Brown and Irber 2016). At a scaled value of 2000, an average of one k-mer will be detected in each 2000 base pair window, and 99.8% of 10,000 base pair windows will have at least one k-mer representative. We selected a k-mer size of 31 because of its species-level specificity (Koslicki and Falush 2016). A signature is composed of hashes, where each hash represents a k-mer contained in the original sequence. We retained all hashes that were present in multiple samples, and refer to these as filtered signatures.

Principle Coordinates Analysis

We used jaccard distance and cosine distance implemented in `sourmash compare` to pairwise compare filtered signatures. We then used the `dist()` function in base R to compute distance matrices. We used the `cmdscale()` function to perform principle coordinate analysis (Gower 1966). We used `ggplot2` and `ggMarginal` to visualize the principle coordinate analysis (Wickham et al. 2019). To test for sources of variation in these distance matrices, we performed PERMANOVA using the `adonis` function in the R `vegan` package (Oksanen et al. 2010). The PERMANOVA was modeled as `~ diagnosis + study accession + library size + number of hashes`.

Random forest classification

We built a random forest classifier to predict CD, UC, and non-IBD status using filtered signatures. First, we transformed sourmash signatures into a hash abundance table where each metagenome was a sample, each hash was a feature, and abundances were recorded for each hash for each sample. We normalized abundances by dividing by the total number of hashes in each filtered signature. We then used a leave-one-study-out validation approach where we trained six models, each of which was trained on five studies and validated on the sixth. To build each model, we first performed vita variable selection on the training set as implemented in the `Pomona` and `ranger` packages (Degenhardt, Seifert, and Szymczak 2017; Wright and Ziegler 2015). Vita variable selection reduces the number of variables (e.g. hashes) to a smaller set of predictive variables through selection of variables with high cross-validated permutation variable importance (Janitza, Celik, and Boulesteix 2018). Using this smaller set of hashes, we then built an optimized random forest model using `tuneRanger` (Probst, Wright, and Boulesteix 2019). We evaluated each validation set using the optimal model, and extracted variable importance measures for each hash for subsequent analysis. To make variable importance measures comparable across models, we normalized importance to 1 by dividing variable importance by the total number of hashes in a model and the total number of models.

213 Characterization of predictive k-mers

214 We used sourmash **gather** with parameters `k 31` and `--scaled 2000` to anchor predictive hashes
215 to known genomes (Brown and Irber 2016). Sourmash **gather** searches a database of known
216 k-mers for matches with a query (Pierce et al. 2019). We used the sourmash GenBank database
217 (2018.03.29, <https://osf.io/snphy/>), and built three additional databases from medium- and high-
218 quality metagenome-assembled genomes from three human microbiome metagenome reanalysis
219 efforts (<https://osf.io/hza89/>) (Pasolli et al. 2019; Nayfach et al. 2019; Almeida et al. 2019).
220 In total, approximately 420,000 microbial genomes and metagenome-assembled genomes were
221 represented by these four databases. We used the sourmash `lca` commands against the GTDB
222 taxonomy database to taxonomically classify the genomes that contained predictive hashes. To
223 calculate the cumulative variable importance attributable to a single genome, we used an iterative
224 winner-takes-all approach. The genome with the largest fraction of predictive k-mers won the
225 variable importance for all hashes contained within its genome. These hashes were then removed,
226 and we repeated the process for the genome with the next largest fraction of predictive k-mers.

227 To identify hashes that were predictive in at least five of six models, we took the union of predictive
228 hashes from all combinations of five models, as well as from the union of all six models. We refer
229 to these hashes as shared predictive hashes. We anchored variable importance of these shared
230 predictive hashes to known genomes using sourmash **gather** as above.

231 Compact de Bruijn graph queries for predictive genomes

232 We used spacegraphcats **search** to retrieve k-mers in the compact de Bruijn graph neighborhood
233 of the genomes that matched predictive k-mers (CITATION). We then used spacegraphcats
234 **extract_reads** to retrieve the reads and **extract_contigs** to retrieve unitigs in the compact de
235 Bruijn graph that contained those k-mers, respectively.

236 Characterization of graph pangenomes

237 **Pangenome signatures** To evaluate the k-mers recovered by pangenome neighborhood queries,
238 we generated sourmash signatures from the unitigs in each query neighborhood. We merged
239 signatures from the same query genome, producing 41 pangenome signatures. We indexed these
240 signatures to create a sourmash gather database. To estimate how query neighborhoods increased
241 the identifiable fraction of predictive hashes, we ran sourmash **gather** with the pangenome
242 database, as well as the GenBank and human microbiome metagenome databases. To estimate
243 how query neighborhoods increased the identifiable fraction of shared predictive hashes, we ran
244 sourmash **gather** with the pangenome database alone. We anchored variable importance of the
245 shared predictive hashes to known genomes using sourmash **gather** results as above.

246 **Differential abundance** We used differential abundance analysis to determine which protein
247 sequences in each pangenome were differentially abundant in IBD subtype. We used `diginorm` on
248 each spacegraphcats query neighborhood implemented in `khmer` as `normalize-by-median.py`
249 with parameters `-k 20 -C 20` (Crusoe et al. 2015). We then combined all query neighborhoods
250 from a single query and used Plass **assemble** with parameter `--min-length 25` to assemble each
251 pangenome in amino acid space (Steinegger, Mirdita, and Söding 2019). We used CD-HIT
252 to cluster amino acid sequences within a pangenome at 90% identity and retained the representative
253 sequence (Fu et al. 2012). To generate amino acid abundance for each metagenome sample for
254 each pangenome, we used `paladin` to align query neighborhood reads to the pangenome amino
255 acid representative sequences, and then used `Salmon` to quantify the number of reads aligned to
256 each amino acid sequence (Westbrook et al. 2017; Patro 2020). Using these abundances, we used
257 the R package `corncob` to perform differential abundance analysis between IBD subtype, using
258 the likelihood ratio test with the formula `study_accession + diagnosis` and the null formula

259 **study_accession** (Martin et al. 2020). We considered amino acid sequences with p values < .05
 260 after bonferonni correction as statistically significant.

261 **Annotation of differentially abundant proteins** We used KofamScan to assign KEGG
 262 ortholog identifiers to each differentially abundant protein, and performed enrichment analysis
 263 using the R package clusterProfiler (Aramaki et al. 2020; Yu et al. 2012).

264 References

- 265 Almeida, Alexandre, Alex L Mitchell, Miguel Boland, Samuel C Forster, Gregory B Gloor,
 266 Aleksandra Tarkowska, Trevor D Lawley, and Robert D Finn. 2019. "A New Genomic Blueprint
 267 of the Human Gut Microbiota." *Nature* 568 (7753): 499.
- 268 Aramaki, Takuya, Romain Blanc-Mathieu, Hisashi Endo, Koichi Ohkubo, Minoru Kanehisa,
 269 Susumu Goto, and Hiroyuki Ogata. 2020. "KofamKOALA: KEGG Ortholog Assignment Based
 270 on Profile Hmm and Adaptive Score Threshold." *Bioinformatics* 36 (7): 2251–2.
- 271 Bolger, Anthony M, Marc Lohse, and Bjoern Usadel. 2014. "Trimmomatic: A Flexible Trimmer
 272 for Illumina Sequence Data." *Bioinformatics* 30 (15): 2114–20.
- 273 Breitwieser, Florian P, Jennifer Lu, and Steven L Salzberg. 2019. "A Review of Methods and
 274 Databases for Metagenomic Classification and Assembly." *Briefings in Bioinformatics* 20 (4):
 275 1125–36.
- 276 Brown, C Titus, and Luiz Irber. 2016. "Sourmash: A Library for Minhash Sketching of Dna." *J.*
 277 *Open Source Software* 1 (5): 27.
- 278 Bushnell, Brian. 2014. "BBMap: A Fast, Accurate, Splice-Aware Aligner." Lawrence Berkeley
 279 National Lab.(LBNL), Berkeley, CA (United States).
- 280 Crusoe, Michael R, Hussien F Alameldin, Sherine Awad, Elmar Boucher, Adam Caldwell, Reed
 281 Cartwright, Amanda Charbonneau, et al. 2015. "The Khmer Software Package: Enabling Efficient
 282 Nucleotide Sequence Analysis." *F1000Research* 4.
- 283 Degenhardt, Frauke, Stephan Seifert, and Silke Szymczak. 2017. "Evaluation of Variable Selection
 284 Methods for Random Forests and Omics Data Sets." *Briefings in Bioinformatics* 20 (2): 492–503.
- 285 Franzosa, Eric A, Xochitl C Morgan, Nicola Segata, Levi Waldron, Joshua Reyes, Ashlee M
 286 Earl, Georgia Giannoukos, et al. 2014. "Relating the Metatranscriptome and Metagenome of the
 287 Human Gut." *Proceedings of the National Academy of Sciences* 111 (22): E2329–E2338.
- 288 Franzosa, Eric A, Alexandra Sirota-Madi, Julian Avila-Pacheco, Nadine Fornelos, Henry J Haiser,
 289 Stefan Reinker, Tommi Vatanen, et al. 2019. "Gut Microbiome Structure and Metabolic Activity
 290 in Inflammatory Bowel Disease." *Nature Microbiology* 4 (2): 293.
- 291 Fu, Limin, Beifang Niu, Zhengwei Zhu, Sitao Wu, and Weizhong Li. 2012. "CD-Hit: Accelerated
 292 for Clustering the Next-Generation Sequencing Data." *Bioinformatics* 28 (23): 3150–2.
- 293 Gevers, Dirk, Subra Kugathasan, Lee A Denson, Yoshiki Vázquez-Baeza, Will Van Treuren, Boyu
 294 Ren, Emma Schwager, et al. 2014. "The Treatment-Naive Microbiome in New-Onset Crohn's
 295 Disease." *Cell Host & Microbe* 15 (3): 382–92.
- 296 Gower, John C. 1966. "Some Distance Properties of Latent Root and Vector Methods Used in
 297 Multivariate Analysis." *Biometrika* 53 (3-4): 325–38.
- 298 Greenblum, Sharon, Peter J Turnbaugh, and Elhanan Borenstein. 2012. "Metagenomic Systems
 299 Biology of the Human Gut Microbiome Reveals Topological Shifts Associated with Obesity and
 300 Inflammatory Bowel Disease." *Proceedings of the National Academy of Sciences* 109 (2): 594–99.

301 Hall, Andrew Brantley, Moran Yassour, Jenny Sauk, Ashley Garner, Xiaofang Jiang, Timothy
302 Arthur, Georgia K Lagoudas, et al. 2017. “A Novel Ruminococcus Gnavus Clade Enriched in
303 Inflammatory Bowel Disease Patients.” *Genome Medicine* 9 (1): 103.

304 Janitza, Silke, Ender Celik, and Anne-Laure Boulesteix. 2018. “A Computationally Fast Variable
305 Importance Test for Random Forests for High-Dimensional Data.” *Advances in Data Analysis
306 and Classification* 12 (4): 885–915.

307 Koslicki, David, and Daniel Falush. 2016. “MetaPalette: A K-Mer Painting Approach for
308 Metagenomic Taxonomic Profiling and Quantification of Novel Strain Variation.” *MSystems* 1
309 (3): e00020–16.

310 Kostic, Aleksandar D, Ramnik J Xavier, and Dirk Gevers. 2014. “The Microbiome in Inflammatory
311 Bowel Disease: Current Status and the Future Ahead.” *Gastroenterology* 146 (6): 1489–99.

312 Lewis, James D, Eric Z Chen, Robert N Baldassano, Anthony R Otley, Anne M Griffiths, Dale
313 Lee, Kyle Bittinger, et al. 2015. “Inflammation, Antibiotics, and Diet as Environmental Stressors
314 of the Gut Microbiome in Pediatric Crohn’s Disease.” *Cell Host & Microbe* 18 (4): 489–500.

315 Lloyd-Price, Jason, Cesar Arze, Ashwin N Ananthakrishnan, Melanie Schirmer, Julian Avila-
316 Pacheco, Tiffany W Poon, Elizabeth Andrews, et al. 2019. “Multi-Omics of the Gut Microbial
317 Ecosystem in Inflammatory Bowel Diseases.” *Nature* 569 (7758): 655.

318 Martin, Bryan D, Daniela Witten, Amy D Willis, and others. 2020. “Modeling Microbial
319 Abundances and Dysbiosis with Beta-Binomial Regression.” *Annals of Applied Statistics* 14 (1):
320 94–115.

321 Morgan, Xochitl C, Timothy L Tickle, Harry Sokol, Dirk Gevers, Kathryn L Devaney, Doyle V
322 Ward, Joshua A Reyes, et al. 2012. “Dysfunction of the Intestinal Microbiome in Inflammatory
323 Bowel Disease and Treatment.” *Genome Biology* 13 (9): R79.

324 Nayfach, Stephen, Zhou Jason Shi, Rekha Seshadri, Katherine S Pollard, and Nikos C Kyrpides.
325 2019. “New Insights from Uncultivated Genomes of the Global Human Gut Microbiome.” *Nature*
326 568 (7753): 505.

327 Oksanen, Jari, F Guillaume Blanchet, Roeland Kindt, Pierre Legendre, RB O’hara, Gavin L
328 Simpson, Peter Solymos, M Henry H Stevens, and Helene Wagner. 2010. “Vegan: Community
329 Ecology Package. R Package Version 1.17-4.” *Http://Cran. R-Project. Org>. Acesso Em* 23:
330 2010.

331 Olson, Nathan D, Todd J Treangen, Christopher M Hill, Victoria Cepeda-Espinoza, Jay Ghurye,
332 Sergey Koren, and Mihai Pop. 2017. “Metagenomic Assembly Through the Lens of Validation: Re-
333 cent Advances in Assessing and Improving the Quality of Genomes Assembled from Metagenomes.”
334 *Briefings in Bioinformatics*.

335 Pasolli, Edoardo, Francesco Asnicar, Serena Manara, Moreno Zolfo, Nicolai Karcher, Federica
336 Armanini, Francesco Beghini, et al. 2019. “Extensive Unexplored Human Microbiome Diversity
337 Revealed by over 150,000 Genomes from Metagenomes Spanning Age, Geography, and Lifestyle.”
338 *Cell* 176 (3): 649–62.

339 Patro, Rob. 2020. *GitHub*. <https://github.com/taylorreiter/2020-aa-abund/issues/1#issue-561732708>.
340 561732708.

341 Pierce, N Tessa, Luiz Irber, Taylor Reiter, Phillip Brooks, and C Titus Brown. 2019. “Large-Scale
342 Sequence Comparisons with Sourmash.” *F1000Research* 8.

343 Probst, Philipp, Marvin N Wright, and Anne-Laure Boulesteix. 2019. “Hyperparameters and
344 Tuning Strategies for Random Forest.” *Wiley Interdisciplinary Reviews: Data Mining and
345 Knowledge Discovery* 9 (3): e1301.

346 Qin, Junjie, Ruiqiang Li, Jeroen Raes, Manimozhiyan Arumugam, Kristoffer Solvsten Burgdorf,
347 Chaysavanh Manichanh, Trine Nielsen, et al. 2010. "A Human Gut Microbial Gene Catalogue
348 Established by Metagenomic Sequencing." *Nature* 464 (7285): 59.

349 Qin, Junjie, Yingrui Li, Zhiming Cai, Shenghui Li, Jianfeng Zhu, Fan Zhang, Suisha Liang, et al.
350 2012. "A Metagenome-Wide Association Study of Gut Microbiota in Type 2 Diabetes." *Nature*
351 490 (7418): 55.

352 Rowe, Will PM. 2019. "When the Levee Breaks: A Practical Guide to Sketching Algorithms for
353 Processing the Flood of Genomic Data." *Genome Biology* 20 (1): 199.

354 Sabatti, Chiara, Lars Rohlin, Min-Kyu Oh, and James C Liao. 2002. "Co-Expression Pattern
355 from Dna Microarray Experiments as a Tool for Operon Prediction." *Nucleic Acids Research* 30
356 (13): 2886–93.

357 Schirmer, Melanie, Ashley Garner, Hera Vlamakis, and Ramnik J Xavier. 2019. "Microbial Genes
358 and Pathways in Inflammatory Bowel Disease." *Nature Reviews Microbiology* 17 (8): 497–511.

359 Seifert, Stephan, Sven Gundlach, and Silke Szymczak. 2019. "Surrogate Minimal Depth as an
360 Importance Measure for Variables in Random Forests." *Bioinformatics* 35 (19): 3663–71.

361 Steinegger, Martin, Milot Mirdita, and Johannes Söding. 2019. "Protein-Level Assembly Increases
362 Protein Sequence Recovery from Metagenomic Samples Manyfold." *Nature Methods* 16 (7): 603–6.

363 Stuart, Joshua M, Eran Segal, Daphne Koller, and Stuart K Kim. 2003. "A Gene-Coexpression
364 Network for Global Discovery of Conserved Genetic Modules." *Science* 302 (5643): 249–55.

365 Thomas, Andrew Maltez, and Nicola Segata. 2019. "Multiple Levels of the Unknown in Microbiome
366 Research." *BMC Biology* 17 (1): 48.

367 Vollmers, John, Sandra Wiegand, and Anne-Kristin Kaster. 2017. "Comparing and Evaluating
368 Metagenome Assembly Tools from a Microbiologist's Perspective-Not Only Size Matters!" *PloS*
369 *One* 12 (1): e0169662.

370 Westbrook, Anthony, Jordan Ramsdell, Taruna Schuelke, Louisa Normington, R Daniel Bergeron,
371 W Kelley Thomas, and Matthew D MacManes. 2017. "PALADIN: Protein Alignment for
372 Functional Profiling Whole Metagenome Shotgun Data." *Bioinformatics* 33 (10): 1473–8.

373 Wickham, Hadley, Mara Averick, Jennifer Bryan, Winston Chang, Lucy McGowan, Romain
374 François, Garrett Grolemund, et al. 2019. "Welcome to the Tidyverse." *Journal of Open Source*
375 *Software* 4 (43): 1686.

376 Wirbel, Jakob, Paul Theodor Pyl, Ece Kartal, Konrad Zych, Alireza Kashani, Alessio Milanese,
377 Jonas S Fleck, et al. 2019. "Meta-Analysis of Fecal Metagenomes Reveals Global Microbial
378 Signatures That Are Specific for Colorectal Cancer." *Nature Medicine* 25 (4): 679.

379 Wright, Marvin N, and Andreas Ziegler. 2015. "Ranger: A Fast Implementation of Random
380 Forests for High Dimensional Data in C++ and R." *arXiv Preprint arXiv:1508.04409*.

381 Yu, Guangchuang, Li-Gen Wang, Yanyan Han, and Qing-Yu He. 2012. "ClusterProfiler: An
382 R Package for Comparing Biological Themes Among Gene Clusters." *Omics: A Journal of*
383 *Integrative Biology* 16 (5): 284–87.